

Review

A Review of Chaotic Systems Based on Memristive Hopfield Neural Networks

Hairong Lin ¹, Chunhua Wang ^{1,*}, Fei Yu ², Jingru Sun ¹, Sichun Du ¹, Zekun Deng ¹ and Quanli Deng ¹¹ College of Computer Science and Electronic Engineering, Hunan University, Changsha 410082, China² School of Computer and Communication Engineering, Changsha University of Science and Technology, Changsha 410114, China

* Correspondence: wch1227164@hnu.edu.cn

Abstract: Since the Lorenz chaotic system was discovered in 1963, the construction of chaotic systems with complex dynamics has been a research hotspot in the field of chaos. Recently, memristive Hopfield neural networks (MHNNs) offer great potential in the design of complex, chaotic systems because of their special network structures, hyperbolic tangent activation function, and memory property. Many chaotic systems based on MHNNs have been proposed and exhibit various complex dynamical behaviors, including hyperchaos, coexisting attractors, multistability, extreme multistability, multi-scroll attractors, multi-structure attractors, and initial-offset coexisting behaviors. A comprehensive review of the MHNN-based chaotic systems has become an urgent requirement. In this review, we first briefly introduce the basic knowledge of the Hopfield neural network, memristor, and chaotic dynamics. Then, different modeling methods of the MHNN-based chaotic systems are analyzed and discussed. Concurrently, the pioneering works and some recent important papers related to MHNN-based chaotic systems are reviewed in detail. Finally, we survey the progress of MHNN-based chaotic systems for application in various scenarios. Some open problems and visions for the future in this field are presented. We attempt to provide a reference and a resource for both chaos researchers and those outside the field who hope to apply chaotic systems in a particular application.

Keywords: chaotic systems; memristor; Hopfield neural network; dynamical behavior; memristor synapse; electromagnetic induction; image encryption

MSC: 34H10; 65P20; 34C23; 68T07



Citation: Lin, H.; Wang, C.; Yu, F.; Sun, J.; Du, S.; Deng, Z.; Deng, Q. A Review of Chaotic Systems Based on Memristive Hopfield Neural Networks. *Mathematics* **2023**, *11*, 1369. <https://doi.org/10.3390/math11061369>

Academic Editor: Daniel-Ioan Curiaç

Received: 13 February 2023

Revised: 6 March 2023

Accepted: 9 March 2023

Published: 11 March 2023



Copyright: © 2023 by the authors. Licensee MDPI, Basel, Switzerland. This article is an open access article distributed under the terms and conditions of the Creative Commons Attribution (CC BY) license (<https://creativecommons.org/licenses/by/4.0/>).

1. Introduction

Chaos theory is an important discovery of human natural science in the 20th century, which is considered the third revolution of basic science after relativity and quantum theory. Chaotic behavior, which is a type of dynamical behavior, was first observed in meteorology to describe the unpredictability of weather [1]. After that, chaos phenomena are found to be widely existent in many natural and non-natural behaviors, such as biotic population [2], road traffic [3], and the stock market [4]. After half a century of in-depth study, chaos has been found to be very useful and has great potential in many disciplines such as mathematics [5], physics [6], chemistry [7], economics [8], information and computer sciences [9], and so on [10,11]. Over the past decades, scholars have devoted great enthusiasm to chaos generation, and a large number of different types of chaotic systems have been constructed.

In the early days, chaos researchers focused mainly on the design of double-scroll/wing chaotic systems. Since Lorenz presented the first chaotic system with double-wing attractors in 1963 [1], many double-scroll/wing chaotic systems have been developed, such as Chua's system [12], Sprott system [13], Jerk system [14], Chen system [15], Lü system [16], and their modified systems [17–21]. These chaotic systems have greatly promoted the development of chaos theory. With further study on the double-scroll/wing chaotic systems, Suykens and Vandewalle [22], in 1993, constructed the first multi-scroll chaotic

systems by introducing a multi-piecewise-linear function into a Chua's circuit. From then on, the design of multi-scroll/wing chaotic systems (MS/WCSs) has greatly stimulated the researchers' interest. During this period, Yu et al. [23–26] proposed a series of nonlinear polynomial function control methods to realize different MS/WCSs based on double-scroll/wing chaotic systems. Afterward, the theory of MS/WCSs has been developed rapidly, and various MS/WCSs such as Lorenz-system-based MS/WCSs [27–29], Chua's-system-based MS/WCSs [30–32], Sprott-system-based MS/WCSs [33–35], Jerk-system-based MS/WCSs [36–38], Chen-system-based MS/WCSs [39,40], and so on [41–47], have been designed using function control methods. However, recent explorations seem to indicate that it is difficult to make new progress in the design of the MS/WCSs.

Renewed research interest in the design of chaotic systems was generated when a physical nonlinear memristor device was first manufactured in 2008 by Hewlett-Packard Lab [48]. Memristor is a nonlinear element that has many special properties, including programmability, nonlinearity, and memory function [49,50]. Due to the special nonlinearity and memory effect, memristors are often used to construct memristive chaotic systems [51,52]. It is found that memristive chaotic systems have the ability to generate complex dynamical behaviors, especially coexisting behaviors [53] and multistability [54]. Furthermore, the memristive chaotic systems have some advantages in solving dynamic equations [55,56]. Therefore, many scholars have developed a great interest in designing memristive chaotic systems in the past decade. In this endeavor, there are three major efforts: (1) constructing memristive chaotic circuits by using the memristors to replace the resistors of the existing chaotic circuits, such as memristor-based Chua's circuit [57,58], memristor-based Jerk circuit [59–62], and so on [63–65]; (2) constructing memristive chaotic systems by introducing memristors into the existing chaotic systems, such as memristor-based double-scroll/wing chaotic systems [66–69], memristor-based multi-scroll/wing chaotic systems [70–78], and so on [79,80]; (3) constructing memristive chaotic systems based on different memristor models, such as memristive chaotic systems [81–87], memristive hyperchaotic systems [88–95], and so on [96–98]. Consequently, the memristive chaotic systems have made extraordinary development, which greatly enriches chaos theory.

In recent years, memristive Hopfield neural networks (MHNNs) with complex, chaotic dynamics have attracted much attention from scholars in the chaos field. The Hopfield neural network presented in 1984 is a brain-like neural network [99], which can exhibit abundant dynamical behaviors, especially chaos [100–106]. Thanks to the inherent memory effect and charge flux relationship, the memristor can be applied in Hopfield neural networks to emulate biological neural synapses or to describe electromagnetic induction effects [107–110]. As a result, a large number of MHNNs have been proposed based on these strategies. It is found that the MHNNs can exhibit complex, chaotic dynamics due to the introduction of the memristors. For example, in 2014, Li et al. [111] constructed the first hyperchaotic MHNN. In 2016, Pham et al. [112] presented the first MHNN with hidden attractors. In 2017, Bao et al. [113] proposed the first MHNN with coexisting attractors. In 2018, Hu et al. [114] presented the first MHNN with hidden coexisting attractors. In 2020, Lin et al. [115] constructed the first MHNN with coexisting infinite attractors. In the same year, Zhang et al. [116] designed the first MHNN with initial-offset behaviors and multi-scroll attractors. In 2022, Lin et al. [117] presented the first MHNN with multi-structure attractors. At the same time, due to their complex dynamics, the MHNNs have wide applications in information encryption and communication security [118–120], especially in the medical image encryption field [121]. Numerous works show that MHNN-based medical encryption schemes have much higher security [122,123]. Therefore, the design of chaotic systems based on MHNNs is becoming a new research hotspot. So far, there have been many important achievements in MHNN-based chaotic systems. However, from the whole research process, the study of the MHNN has just started, and more MHNN-based chaotic systems are still to be explored and discovered. Therefore, a detailed review is needed for the existing chaotic MHNNs. This review aims to address this shortcoming. Compared with the review [108], this review has three advantages: (1) MHNNs are divided into more

types in terms of different functions and positions of memristors in neural networks than just functions; (2) Some important, relevant research results in the last two years have been added; (3) Some of the open questions raised earlier are partially answered in this article.

The rest of this article is organized as follows. In Section 2, some basic knowledge, including HNN, memristor, and chaotic dynamics, is introduced. In Section 3, different modeling methods of the MHNNs are analyzed, and related works are reviewed in detail. MHNN-based application and future work are presented in Section 4. Finally, in Section 5, conclusions are drawn.

2. Introduction of Basic Knowledge

This section first briefly introduces the original model of the Hopfield neural network, then describes the basic concepts and properties of the memristor, and finally gives the basic definitions and classification of the chaotic dynamics.

2.1. Hopfield Neural Networks

Neuroscience shows that the human brain nervous system contains tens of billions of neurons [124]. Neurons are connected to each other by synapses, including chemical and electrical synapses. Each synapse has an adjustable synaptic weight that characterizes the coupling strength between the two neurons. According to these biological principles, the original model of the Hopfield neural network was developed by Hopfield in 1984 [99]. Due to its special network structure and hyperbolic tangent function, the HNN can exhibit abundant dynamical behaviors. The HNN with n neurons can be described by a set of dimensionless nonlinear ordinary differential equations as follows [99]:

$$\dot{\mathbf{x}} = -\mathbf{x} + \mathbf{W}\tanh(\mathbf{x}) + \mathbf{I} \tag{1}$$

where

$$\mathbf{x} = \begin{bmatrix} x_1 \\ x_2 \\ \vdots \\ x_i \\ \vdots \\ x_n \end{bmatrix}, \mathbf{I} = \begin{bmatrix} I_1 \\ I_2 \\ \vdots \\ I_i \\ \vdots \\ I_n \end{bmatrix}, \mathbf{W} = \begin{bmatrix} w_{11} & w_{12} & \cdots & w_{1j} & \cdots & w_{1n} \\ w_{21} & w_{22} & \cdots & w_{2j} & \cdots & w_{2n} \\ \vdots & \vdots & \ddots & \vdots & \vdots & \vdots \\ w_{i1} & w_{i2} & \cdots & w_{ij} & \cdots & w_{in} \\ \vdots & \vdots & \vdots & \vdots & \ddots & \vdots \\ w_{n1} & w_{n2} & \cdots & w_{nj} & \cdots & w_{nn} \end{bmatrix} \tag{2}$$

where x_i denotes the i -neuron membrane voltage, $\tanh(\mathbf{x})$ is the neuron activation function, and I_i represents i -neuron external stimulate current. Furthermore, the \mathbf{W} represents the synaptic weight matrix, where w_{ij} represents the synaptic weight between the j -neuron and to i -neuron. Commonly, the synaptic weight is a resistive synaptic weight that can be achieved by a resistor. Over the past decades, many improved models have been constructed based on the original HNN model, such as HNNs with different active functions [125], HNNs with time delay [126], fractional HNNs [127,128], discrete HNNs [129], and so on [130,131].

2.2. Memristor

In the year 1971, Chua proposed the concept of memristor based on the symmetry theory of circuit variables [132]. The memristor is a memory resistor, which describes the relationship between charge and flux. Later on, the memristor concept is extended to include any two-terminal device with a pinched hysteresis loop that always passes through the origin in the voltage-current plane when triggered by a periodic voltage or current signal [50]. In 2008, Hewlett-Packard Lab manufactured the first physical memristor device [48], which opened up a new research field related to memristors. With the development of memristors, many key memristor theories have been built. According to the memristor theories [49,50], a common ideal flux-controlled memristor model can be written by

$$\begin{cases} i = W(\varphi)v \\ \dot{\varphi} = v \end{cases} \tag{3}$$

where v, i are the input voltage and output current, respectively. $W(\varphi)$ is a continuous function of φ , called the memductance, and φ is the flux. For example, in [53], $W(\varphi) = m + n\varphi^2$, where m and n are constant parameters. Moreover, a generic memristor is defined by

$$\begin{cases} i = W(\varphi)v \\ \dot{\varphi} = f(\varphi, v) \end{cases} \quad (4)$$

where $W(\varphi)$ is the memductance, φ is the memristor state variable, and $f(\varphi, v)$ is called the state equation, which is a Lipschitz function. For instance, in [115], $W(\varphi) = \varphi$ and $f(\varphi, v) = \sin(\varphi) + v$.

In recent years, memristors have been widely investigated and applied in various fields [133–135]. Among them, the memristor is often used to construct memristive neural networks due to its bionic characteristics [136–138]. On the one hand, the memristor can be used to describe electromagnetic induction effects in biological nervous systems because of its characteristic of magnetic flux [139,140]. On the other hand, the memristor can be used to emulate neural synapses in nervous systems [141,142].

2.3. Chaotic Dynamics

Chaotic behavior is a type of special dynamical behavior that has many unique properties, such as initial state sensitivity, unpredictability, ergodicity, and topological mixing [1–4]. Over the past few decades, many methods have been proposed to study chaotic dynamics, such as equilibrium point stability, bifurcation diagrams, Lyapunov exponents, phase portraits, Poincare maps, basins of attraction, and so on. In order to better reveal dynamical behavior in chaotic systems, chaotic dynamics with different characteristics are classified and studied. From the perspective of Lyapunov exponents, chaotic dynamics can be divided into chaos, transient chaos, and hyperchaos. Usually, a dynamical behavior with at least one positive Lyapunov exponent on infinite time is considered chaos [12–15]. Transient chaos is a dynamical behavior that the existence of chaos is on finite time [143]. Hyperchaos [88–90], which is more complicated than chaos and transient chaos, is defined as chaos with two or more positive Lyapunov exponents. From the perspective of equilibrium point stability, the chaotic dynamics include self-excited attractors and hidden attractors [144]. If an attractor's basin of attraction does not intersect with any open neighborhood of the system equilibria, it is referred to as a hidden attractor. Otherwise, it is referred to as a self-excited attractor. From the perspective of attractor structure, chaotic dynamics contain single-scroll/wing attractors and multi-scroll/wing attractors [23–26]. The multi-scroll/wing attractors have multiple single-scroll/wing chaos trajectories. Generally, multi-scroll/wing attractors are more complex compared to single-scroll/wing attractors. From the perspective of stability, chaotic dynamics contain coexisting attractors [53], multistability [62], and extreme multistability [58]. The complex dynamical phenomenon of coexisting attractors consists of two distinct types of chaotic behaviors in two different initial conditions. Multistability refers to the simultaneous existence of three or more dynamical behaviors in distinct initial conditions. Multistability implies that a rich variety of stable states exists in chaotic systems, which mirrors the qualities of complex systems. There are two special types of systems with multistability: extreme multistability systems and megastable systems [145]. Extreme multistability is the term for the phenomenon in which infinitely many coexisting attractors. Additionally, the phenomenon of the coexistence of infinite attractors with the same topology structures and different positions is called initial-offset coexisting behaviors [146].

3. Memristive Hopfield Neural Networks

In this section, the MHNNs are divided into four categories according to the different functions and positions of memristors in neural networks. The modeling mechanism of each category is analyzed, and existing MHNN-based chaotic systems are reviewed and introduced.

3.1. Using Memristors to Emulate Neural Synapses

In the traditional HNN model (1), the synaptic weight w_{ij} is a resistive synaptic weight that is realized by using resistors to emulate neural synapses. Compared with

resistors, memristors have many synapse-like properties, including nanoscale, nonlinearity, adjustability, and nonvolatility, which make them more suitable for emulating neural synapses. Therefore, when using the memristors to simulate the neural synapses in the traditional HNN model, the memristive HNN model can be constructed [108]. That is to say that when the resistive synaptic weight w_{ij} is replaced with the memristive synaptic weight $W(\varphi)$, the MHNN is modeled. Due to the introduction of the memristive synaptic weight, the MHNN model is closer to the biological nervous system. As a result, the MHNN can generate more complex dynamical behaviors. Generally, the biological nervous system has two types of neural synapses, namely self-connection autapses and coupling synapses. For the HNN model, there are two types of synaptic weights, namely self-connection synaptic weights w_{ij} ($i = j$) and coupling synaptic weights w_{ij} ($i \neq j$). Therefore, according to different types of memristor synapses, the MHNN can be divided into two categories: memristor-autapse-based MHNN and memristor-synapse-based MHNN.

Category 1: Memristor-autapse-based MHNNs

The models of the memristor-autapse-based MHNNs can be constructed by replacing resistive self-connection synaptic weights with memristive self-connection synaptic weights. Taking $n = 3$ as an example, the connection topology for the memristor-autapse-based MHNN with a memristor autapse is shown in Figure 1. As shown in Figure 1, we replace resistive self-connection synaptic weight w_{22} with the memristive self-connection synaptic weight $W(\varphi)$, and then the original HNN model has an additional differential equation about φ . Thus, its mathematical model can be described in a dimensionless form as

$$\begin{cases} \dot{\mathbf{x}} = -\mathbf{x} + \mathbf{W}\tanh(\mathbf{x}) + \mathbf{I} \\ \dot{\varphi} = f(\varphi, v_i) \end{cases} \tag{5}$$

where

$$\mathbf{x} = \begin{pmatrix} x_1 \\ x_2 \\ x_3 \end{pmatrix}, \mathbf{I} = \begin{pmatrix} I_1 \\ I_2 \\ I_3 \end{pmatrix}, \mathbf{W} = \begin{bmatrix} w_{11} & w_{12} & w_{13} \\ w_{21} & W(\varphi) & w_{23} \\ w_{31} & w_{32} & w_{33} \end{bmatrix} \tag{6}$$

where x_i is the membrane potential of the i -neuron, and $\tanh(x_i)$ represents the neuron activity function.

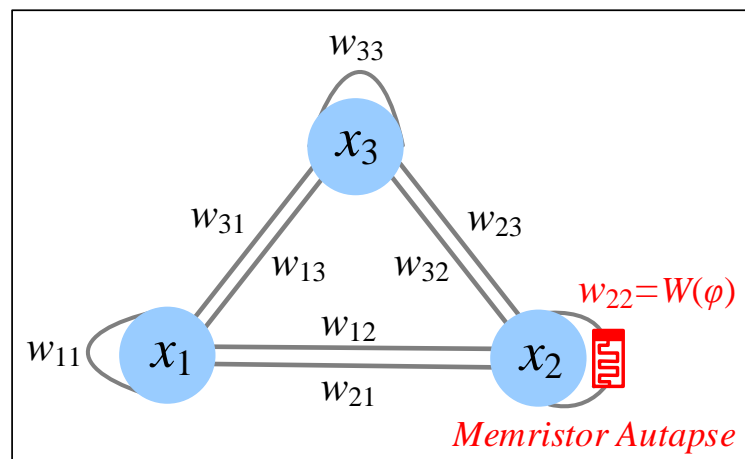


Figure 1. Connection topology of a memristor-autapse-based MHNN.

Over the past years, many different MHNNs with memristor autapses have been constructed, and various chaotic dynamical behaviors have been revealed. For example, Ref. [147] proposed an MHNN model with three neurons by using hyperbolic-type memristor autapses to replace resistor autapses. The authors found that the MHNN can generate abundant dynamical behaviors, including chaos, coexisting attractors, and the Feigenbaum tree. Ref. [148] constructed an MHNN with two neurons by introducing a linear memristor autapse, and bursting firing and chaos were observed. Initial offset coexisting behaviors

and multi-double-scroll attractors have been reported in an MHNN with a multi-piecewise quadratic nonlinearity memristor autapse [116]. Concurrently, some similar MHNNs with multi-scroll chaotic attractors have been reported in [149,150]. By considering memristive self-connection synaptic weight, an MHNN with one neuron has been proposed [151]. Numerical analysis and experimental results show that the MHNN with one neuron can generate multiple firing behaviors like coexisting periodic and chaotic spiking, chaotic bursting, and periodic bursting. Moreover, hidden extreme multistability has been found in a one-neuron-based MHNN with cosine memristor autapse [152]. Infinitely many coexisting hidden attractors have been reported in a two-neuron-based MHNN with a modified hyperbolic-type memristor autapse [153]. In particular, recently, Ref. [154] proposed an MHNN with two memristor autapses. The authors found that the MHNN can exhibit complex initial-offset plane coexisting behaviors. Additionally, the MHNN with multiple memristor autapses has also been investigated [155]. The research results show that with the increase of memristor autapses, the MHNN can generate different dynamical behaviors like exciting neurodynamics or inhibiting neurodynamics.

Category 2: Memristor-synapse-based MHNNs

The model of the memristor-synapse-based MHNNs can be constructed by replacing resistive coupling synaptic weights with memristive coupling synaptic weights. Taking $n = 3$ as an example, the connection topology for the memristor-synapse-based MHNN with a memristor synapse is shown in Figure 2. As shown in Figure 2, we replace a resistive coupling synaptic weight w_{12} with a memristive coupling synaptic weight $W(\varphi)$, and then the original HNN model has an additional differential equation about φ . Thus, its mathematical model can be described in a dimensionless form as

$$\begin{cases} \dot{\mathbf{x}} = -\mathbf{x} + \mathbf{W}\tanh(\mathbf{x}) + \mathbf{I} \\ \dot{\varphi} = f(\varphi, v_j) \end{cases} \tag{7}$$

where

$$\mathbf{x} = \begin{pmatrix} x_1 \\ x_2 \\ x_3 \end{pmatrix}, \mathbf{I} = \begin{pmatrix} I_1 \\ I_2 \\ I_3 \end{pmatrix}, \mathbf{W} = \begin{bmatrix} w_{11} & w_{12} & w_{13} \\ W(\varphi) & w_{22} & w_{23} \\ w_{31} & w_{32} & w_{33} \end{bmatrix} \tag{8}$$

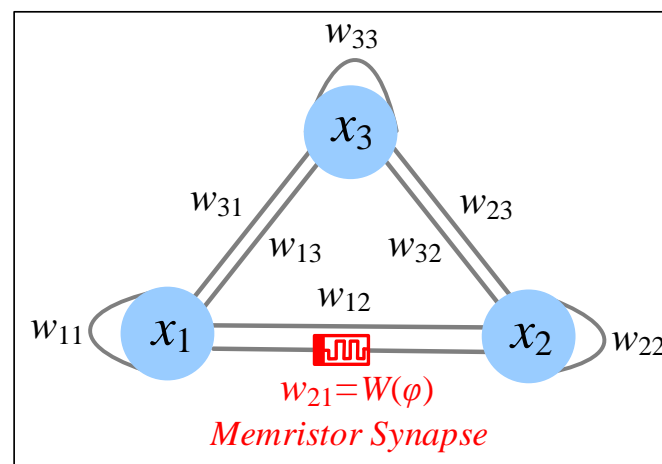


Figure 2. Connection topology of a memristor-synapse-based MHNN.

In recent years, various MHNNs with memristor synapses have been reported. Dynamical analysis and numerical simulation showed that MHNNs could generate complex, chaotic dynamical behaviors. For instance, Ref. [111] proposed an MHNN with three neurons by using a memristive coupling synaptic weight to substitute a resistive coupling synaptic weight. The proposed MHNN can generate hyperchaotic behavior. Hidden attractors have been revealed in a three-neuron-based MHNN with a quadratic memristor synapse [112]. Based on a hyperbolic-type memristor synapse, Ref. [113] found that the

MHNN with three neurons can generate coexisting asymmetric attractors. Particularly, Ref. [156] has shown that the MHNN with an improved hyperbolic-type memristor synapse can exhibit chimera state, synchronization, and oscillation death. Infinitely many coexisting attractors have been observed in a four-neuron-based MHNN with a multi-stable memristor synapse [115]. In [157], a fraction-order MHNN with a hyperbolic-type memristor synapse is proposed. Research results show that the fraction-order MHNN can generate complex dynamical transition, evolving from periodic to chaotic and finally to coexisting attractors. Complete synchronization and anti-phase synchronization have been investigated in two coupled MHNNs with a hyperbolic-type memristor synapse [158]. Considering the influence of synaptic cross-talk in the MHNN with three neurons, multi-stability, asymmetry attractors, and anti-monotonicity have been observed in an MHNN with a novel hyperbolic-type memristor synapse [159]. The complex phenomenon of multi-scroll attractors has been found in two different MHNNs [122,160]. The multi-structure attractors have been reported in a four-neuron-based MHNN with different memristor synapses [117]. Initial-offset coexisting behaviors have been revealed in some MHNNs with memristor synapses [161,162]. Furthermore, Ref. [163] designed an MHNN with two generalized multi-stable memristor synapses. The authors found that the MHNN with two memristor synapses can generate chaos and coexisting asymmetric attractors. Such complex dynamical behaviors have been demonstrated on a DSP platform. Similarly, Ref. [164] designed an MHNN with a hyperbolic-type memristor autapse and a hyperbolic-type memristor synapse, which can generate grid multi-scroll attractors. The MHNN with three hyperbolic-type memristor synapses has been investigated in Ref. [165]. Recently, locally active memristors have attracted much attention in the construction of MHNNs due to their synapse-like local activity. Ref. [166] presented an MHNN with three neurons by replacing a coupling synapse with a tristable locally active memristor. It is found that the MHNN can generate complex bursting oscillation and multistability. Ref. [167] proposed a fractional-order MHNN with a locally active memristor synapse. Research results show that the fractional-order MHNN can exhibit the dynamical behavior of the coexistence of multiple attractors. In addition, multi-scroll chaotic attractors have also been observed in an MHNN with a local active memristor synapse [168].

3.2. Using Memristor to Describe Electromagnetic Induction

The traditional HNN model does not consider the influence of electromagnetic induction. In fact, numerous physical and biological experiments show that the biological nervous systems are often affected by the electromagnetic field generated by internal membrane voltages difference and external electromagnetic radiation [107,108]. According to the physical law of electromagnetic induction, the distribution and density of magnetic flux across the membrane can be changed when a neuron is exposed to an electromagnetic field. Consequently, the electrical activities of the biological nervous system can be changed due to the electromagnetic field. To consider the effects of the electromagnetic field on the dynamics of the nervous system, the flux-controlled memristor is introduced into the traditional HNN model to describe the electromagnetic induction current. When the effect of an electromagnetic field on a neuron is considered as magnetic flux across the membrane of the neuron, the coupling between magnetic flux and membrane potential can be described by using a voltage-controlled memristor [109,110]. Consequently, the nervous systems under an electromagnetic field can be modeled by adding a magnetic induction current in the traditional HNN model. That is to say that an MHNN model can be constructed by considering the effect of an electromagnetic field. Usually, according to different types of electromagnetic fields, the MHNNs can be divided into another two categories: MHNNs under external electromagnetic radiation and MHNNs under an internal electromagnetic field.

Category 3: MHNNs under external electromagnetic radiation

When considering neurons are exposed to external electromagnetic radiation, an electromagnetic induction current can be described by a flux-controlled memristor [107,108]. Thus,

the model of the MHNNs under external electromagnetic radiation can be constructed. Taking $n = 3$ as an example, the connection topology of an MHNN under external electromagnetic radiation is given in Figure 3. The mathematical model of the MHNN under electromagnetic radiation can be written as

$$\begin{cases} \dot{\mathbf{x}} = -\mathbf{x} + \mathbf{W}\tanh(\mathbf{x}) + I_M + \mathbf{I} \\ \dot{\varphi} = f(\varphi, x_i) \end{cases} \quad (9)$$

where

$$I_M = \rho W(\varphi)x_i \quad (10)$$

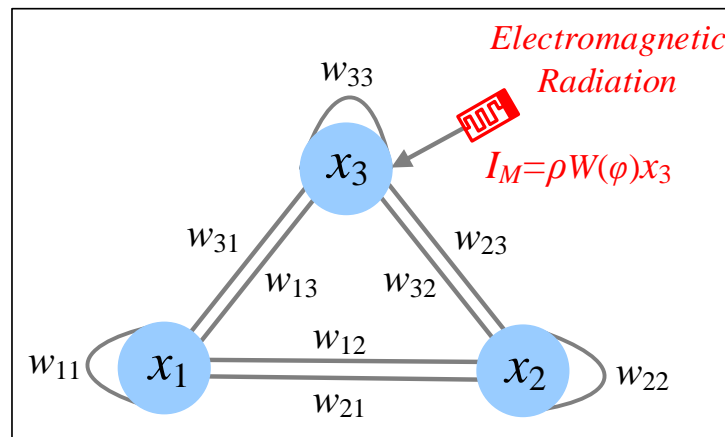


Figure 3. Connection topology of an MHNN under external electromagnetic radiation.

Here the \mathbf{W} represents the synaptic weight matrix, and I_M represents the electromagnetic induction current caused by external electromagnetic radiation. The parameter ρ represents the coupling strength between membrane potential and magnetic flux. $W(\varphi)$ is the memconductance of the flux-controlled memristor, and x_i is the membrane potential of the neuron under electromagnetic radiation. In this case, x_i is the membrane potential x_3 of the 3-neuron.

Based on this model, the influence of external electromagnetic radiation on chaotic dynamical behaviors in neural networks can be analyzed. For example, complex dynamical behaviors, including coexisting chaos and transient chaos, have been revealed in a three-neuron-based MHNN under external electromagnetic radiation [114]. The effects of external electromagnetic radiation distribution on the chaotic dynamical behaviors of a neural network with n neurons are investigated in an MHNN [169]. The authors found that with the increasing number of neurons under external electromagnetic radiation, the dynamical behavior of the MHNN gradually changes from period to chaos, then to transient chaos, and finally to hyperchaos. Hidden extreme multistability with hyperchaos and transient chaos is discussed in a three-neuron-based HNN under external electromagnetic radiation [170]. Multi-scroll attractors [171] and multi-style attractors [172] have been reported in MHNNs under external electromagnetic radiation. Furthermore, Ref. [123] proposed a ring MHNN under external electromagnetic radiation. It is found that the ring MHNN can generate complex hyperchaotic behavior. Additionally, Ref. [173] found that an MHNN under external electromagnetic radiation can exhibit multistable dynamics, including periodic attractors, quasi-periodic attractors, transient chaotic attractors, and hidden chaotic attractors. Additionally, an MHNN with different external stimuli, including electromagnetic radiation and multi-level logic pulse, has been studied in Ref. [174]. The research results demonstrated that the MHNN with multiple external stimuli could generate complex coexisting attractors and multi-scroll attractors.

Category 4: MHNNs under internal electromagnetic field

When possessing a potential difference between two neurons, an internal electromagnetic induction current appears in the neural network, which can be described by a

flux-controlled memristor synapse [107,108]. Thus, the model of the MHNN under an internal electromagnetic field can be constructed. Taking $n = 3$ as an example, a structure diagram of a three-neuron-based MHNN under an internal electromagnetic field is given in Figure 4. As shown in Figure 4, an induced current is sensed by the internal electromagnetic field caused by potential difference $(x_2 - x_3)$ between two neurons in the HNN, which can be characterized by an electromagnetic induction current I_M following through a flux-controlled memristor synapse. Therefore, an MHNN under an internal electromagnetic field is established, which is mathematically described as

$$\begin{cases} \dot{\mathbf{x}} = -\mathbf{x} + \mathbf{W}\tanh(\mathbf{x}) + I_M + \mathbf{I} \\ \dot{\varphi} = f(\varphi, (x_i - x_j)) \end{cases} \quad (11)$$

where

$$I_M = \rho W(\varphi)(x_i - x_j) \quad (12)$$

where ρ represents coupling strength between memristor and neuron, $W(\varphi)$ is a memductance function, $(x_i - x_j)$ is the potential difference between two neurons.

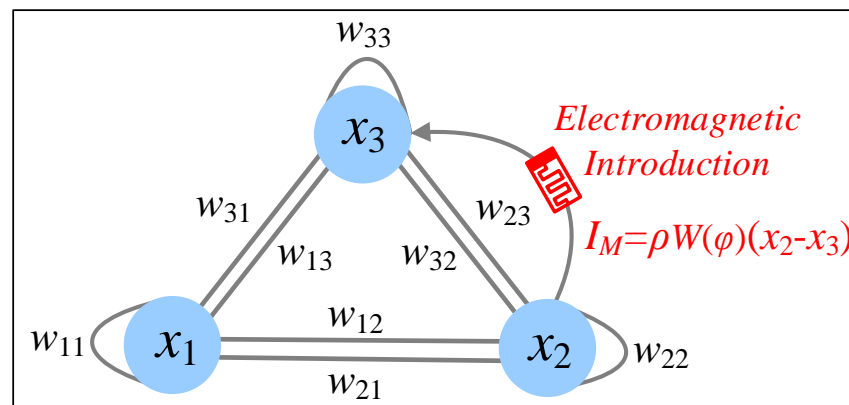


Figure 4. Connection topology of an MHNN under an internal electromagnetic field.

MHNNs under internal electromagnetic fields have been reported in recent years. For example, Ref. [175] proposed a two-neuron-based MHNN by considering an internal electromagnetic induction current. It is found that the MHNN can produce coexisting multi-stable patterns such as spiral chaotic patterns with different dynamic amplitudes, periodic patterns with different periodicities, and stable resting patterns with different positions. Similarly, considering an internal induced current described by a non-ideal memristor synapse, Ref. [176] designed a bi-neuron MHNN with coexisting attractors. The MHNN with different numbers of internal electromagnetic induction currents has been investigated in Ref. [177]. The authors found that when using hyperbolic-type memristors to link different neurons, the MHNN can generate different dynamical behaviors, including periodic and chaotic bubbles, initial-related multistable patterns, and riddled basins of attraction. Utilizing a hyperbolic-type memristor and a quadratic nonlinear memristor to simulate the effects of internal electromagnetic induction and external electromagnetic radiation, a three-neuron-based MHNN with coexisting behaviors has been reported in Ref. [178]. The generation mechanism of chaos has been researched in a ring fraction-order MHNN with an internal electromagnetic induction current [179]. Moreover, the fractional-order MHNN with three internal electromagnetic induction currents has been reported in Ref. [180]. It is found that the fractional-order MHNN can exhibit complex coexisting behaviors. Initial-offset coexisting hyperchaotic attractors have been observed in a coupled MHNN with an induced current [121]. Ref. [181] proposed an MHNN with time delay by using a memristor synapse to emulate the electromagnetically induced current. The complex dynamical behaviors, including coexisting chaos, periodic limit cycles, and stable point attractors, have been revealed in a two-neuron-based MHNN with an internal electromagnetic induction current [182]. Additionally, hyperchaotic multi-

structure attractors have been reported in a memristor-couple asymmetric MHNN with an internal electromagnetic induction current caused by membrane potential difference [118].

To facilitate readers' reading, we summarize different dynamical behaviors in the MHNNs, as shown in Table 1. As can be seen, many complex dynamical behaviors have been revealed from the MHNNs, especially coexisting attractors, hidden attractors, multi-scroll attractors, multistability, extreme multistability, and initial-offset coexisting behaviors. Furthermore, some unfrequent dynamical behaviors, such as the Feigenbaum tree, chimera state, and multi-structure attractors, have also been reported in the MHNNs.

Table 1. Various dynamical behaviors in the MHNNs.

Dynamical Behaviors	References
Transient chaos	[114,169,173]
Hyperchaos	[111,118,123,169]
Feigenbaum tree	[147]
Coexisting attractors	[113,147,157,163,174,176,178,180,182]
Bursting firing	[148,151,166]
Chimera state	[156]
Hidden attractors	[112,152,153,170,173]
Synchronization	[156,158]
Multi-scroll attractors	[116,120,122,149,150,160,164,168,171,172,174,183]
Multi-structure attractors	[117,118]
Multistability	[124,151,155,159,166,167,173,175,177]
Extreme multistability	[115,116,121,152–154,161,162,170]
Hidden extreme multistability	[152,153,170]
Initial-offset coexisting behaviors	[116,121,154,161,162]

4. Application and Future Works

Due to flexible network structure and abundant dynamical behaviors, traditional HNNs have been widely applied in various fields, such as associative memory [101], information protection [102], process optimization [103], and so on [129,130]. Compared with traditional HNN models, the MHNNs have some advantages in terms of chip area, computing speed, and complex dynamical behaviors, which makes them have wider application ranges. For example, Ref. [184] designed a reconfigurable MHNN circuit that can realize associative memory quickly. An efficient combinatorial optimization method has been presented by weight annealing in MHNN [185]. Due to their complex, chaotic dynamical behaviors, the MHNNs can be used to generate random numbers with high randomness. Thus, it is very suitable for information protection and image encryption. For example, Ref. [116] proposed an image encryption scheme based on an MHNN with initial-offset coexisting behaviors. The encryption results show that the proposed encryption scheme has excellent security due to the high randomness of the MHNN. Ref. [186] designed a pseudo-random number generator by using an MHNN with complex, chaotic attractors. At the same time, some image encryption schemes have been presented and verified based on various MHNNs, such as the MHNNs with multi-scroll attractors [150,168,184], the MHNNs with multi-style attractors [172], and the fractional-order MHNN with coexisting attractors [180]. Furthermore, Refs. [118,167] designed color image cryptosystems based on an MHNN with hyperchaotic multi-structure attractors and an MHNN with coexisting multiple attractors, respectively. Additionally, Ref. [183] proposed an audio encryption scheme based on a fractional-order multi-scroll MHNN. Recently, due to their characteristics of artificial intelligence and complex dynamical behaviors, MHNNs have attracted much attention in the field of medical image encryption. For instance, Ref. [121] designed a

biomedical image encryption scheme based on an MHNN with brain-like initial-boosted hyperchaos. Experimental evaluations showed that the designed medical image cryptosystem has some advantages in the keyspace, information entropy, and key sensitivity. Similarly, some other medical image encryption schemes have also been reported based on different MHNNs, such as ring MHNN with hyperchaos [123], MHNN with multi-scroll attractors [122], and MHNN with multi-structure attractors [117]. Moreover, to ensure the information security of the medical data transmitted through the Internet of Things, Ref. [120] proposed a medical data encryption method based on a multi-scroll MHNN.

As reviewed above, the MHNNs with complex, chaotic behaviors have greatly stimulated researchers' interest, and many valuable research results have been reported to date. In particular, some work has answered the questions raised earlier in the review [108]. For example, different from the previous special structure, the MHNNs with ring structure have been proposed in [123,165]. To construct a reliable neural network model, internal electromagnetic induction has been considered in some recent research [175–182]. However, several important questions still remain to be answered. There are at least four aspects that can be further explored. First, it is well known that the nervous system is composed of a large number of neurons. However, the existing MHNN models only consider several neurons, such as two-neuron-based MHNNs [148], three-neuron-based MHNNs [156], and four-neuron-based MHNNs [150]. So, the MHNN with more neurons needs to be further developed and investigated. Second, the biological nervous system has many neural autapses and synapses. So far, the current MHNNs mainly consider a few memristor autapses and memristor synapses, like one-memristor-based MHNNs [162] and two-memristor-based MHNNs [154]. Undoubtedly, the MHNN with multiple memristor autapses and memristor synapses needs to be further designed and researched. Third, the biological nervous system is very sensitive to external stimuli such as electromagnetic radiation, electric field, light, temperature, noise, and so on. At present, other factors are rarely considered in the existing MHNNs besides electromagnetic radiation. Therefore, to model a reliable and realistic neural network model, different external stimuli and internal factors should be added to MHNN models. Fourth, from the viewpoint of chaos-based application, the MHNNs have the features of high dimensional equations, artificial intelligence [187–189], and complex dynamical behaviors [190], which makes them more suitable for application in medical image encryption, video encryption, and pseudo-random number generators. Therefore, MHNN-based applications in information protection can be further discussed in the future. Additionally, most of the current MHNNs are based on the memristor mathematical model. In our opinion, the real nano-memristor is essential if the memristor-based chaotic systems and neural networks are to be applied in practical engineering [191,192]. Undoubtedly, it is a new research direction to construct MHNNs with complex, chaotic dynamics using nano-memristor.

5. Conclusions

In this review, several significant results on MHNN-based chaotic systems are introduced for readers in the field of chaos. First, the basic knowledge of Hopfield neural networks, memristors, and chaotic dynamics is illustrated. Then according to the different functions of the memristors in MHNNs, we divide MHNNs into four different models, namely, the MHNNs with memristor autapses, the MHNNs with memristor synapses, the MHNNs under electromagnetic radiation, and the MHNNs with electromagnetic induction. The modeling mechanism, modeling method, and pioneering works of each type are introduced. Concurrently, we reviewed some recent important papers related to those types. Finally, potential applications of the MHNNs within different areas, especially information encryption, are also introduced, and future work has been discussed. This discussion could be helpful for further investigation of MHNN-based chaotic systems. Although some MHNN-based chaotic systems and their chaotic dynamics have been reported, it is still in the infant stage and needs to be further researched. We hope that this review can provide a good reference for researchers who want to investigate such chaotic systems deeply.

Author Contributions: Conceptualization, H.L. and C.W.; methodology, H.L.; validation, F.Y., J.S. and S.D.; investigation, H.L.; resources, C.W.; data curation, Z.D.; writing—original draft preparation, H.L.; writing—review and editing, C.W. and Q.D.; supervision, F.Y.; project administration, C.W.; funding acquisition, H.L. and C.W. All authors have read and agreed to the published version of the manuscript.

Funding: This work was supported in part by the National Natural Science Foundation of China under Grant 62201204, Grant 62271197, Grant 61971185, and 62171182; in part by the China Postdoctoral Science Foundation under Grant 2022M71104; and in part by the Natural Science Foundation of Hunan Province under Grant 2022JJ30160.

Data Availability Statement: The datasets generated during and/or analyzed during the current study are available from the corresponding author on reasonable request.

Conflicts of Interest: The authors declare no conflict of interest.

References

1. Lorenz, E.N. Deterministic nonperiodic flow. *J. Atmos. Sci.* **1963**, *20*, 130–141. [\[CrossRef\]](#)
2. Huisman, J.; Weissing, F.J. Biodiversity of plankton by species oscillations and chaos. *Nature* **1999**, *402*, 407–410. [\[CrossRef\]](#)
3. Dendrinos, D.S. Traffic-flow dynamics, a search for chaos. *Chaos Solitons Fractals* **1994**, *4*, 605–617. [\[CrossRef\]](#)
4. Kazem, A.; Sharifi, E.; Hussain, F.K.; Saberi, M.; Hussain, O.K. Support vector regression with chaos-based firefly algorithm for stock market price forecasting. *Appl. Soft. Comput.* **2013**, *13*, 947–958. [\[CrossRef\]](#)
5. Gu, H.; Li, C.; Li, Y.; Ge, X.; Lei, T. Various patterns of coexisting attractors in a hyperchaotic map. *Nonlinear Dyn.* **2023**, *111*, 7807–7818. [\[CrossRef\]](#)
6. Sciamanna, M.; Shore, K.A. Physics and applications of laser diode chaos. *Nat. Photonics* **2015**, *9*, 151–162. [\[CrossRef\]](#)
7. Kol'tsov, N.I.; Fedotov, V.K. Two-Dimensional Chaos in chemical reactions. *Russ. J. Phys. Chem. B* **2018**, *12*, 590–592. [\[CrossRef\]](#)
8. Yousefpour, A.; Jahanshahi, H.; Munoz-Pacheco, J.M.; Bekiros, S.; Wei, Z. A fractional-order hyper-chaotic economic system with transient chaos. *Chaos Solitons Fractals* **2020**, *130*, 109400. [\[CrossRef\]](#)
9. Zhu, Y.; Wang, C.; Sun, J.; Yu, F. A chaotic image encryption method based on the artificial fish swarms algorithm and the DNA coding. *Mathematics* **2023**, *11*, 767. [\[CrossRef\]](#)
10. Yu, F.; Zhang, W.; Xiao, X.; Yao, W.; Cai, S.; Zhang, J.; Wang, C.; Li, Y. Dynamic analysis and FPGA implementation of a new, simple 5D memristive hyperchaotic Sprott-C system. *Mathematics* **2023**, *11*, 701. [\[CrossRef\]](#)
11. Lu, Y.M.; Wang, C.H.; Deng, Q.L.; Xu, C. The dynamics of a memristor-based Rulkov neuron with fractional-order difference. *Chin. Phys. B* **2022**, *31*, 060502. [\[CrossRef\]](#)
12. Matsumoto, T. A chaotic attractor from Chua's circuit. *IEEE Trans. Circuits Syst.* **1984**, *31*, 1055–1058. [\[CrossRef\]](#)
13. Sprott, J.C. Some simple chaotic flows. *Phys. Rev. E* **1994**, *50*, R647. [\[CrossRef\]](#) [\[PubMed\]](#)
14. Sprott, J.C. Some simple chaotic jerk functions. *Am. J. Phys.* **1997**, *65*, 537–543. [\[CrossRef\]](#)
15. Chen, G.; Ueta, T. Yet another chaotic attractor. *Int. J. Bifurc. Chaos* **1999**, *9*, 1465–1466. [\[CrossRef\]](#)
16. Lü, J.; Chen, G. A new chaotic attractor coined. *Int. J. Bifurc. Chaos* **2002**, *12*, 659–661. [\[CrossRef\]](#)
17. Li, C.; Chen, G. Chaos in the fractional order Chen system and its control. *Chaos Solitons Fractals* **2004**, *22*, 549–554. [\[CrossRef\]](#)
18. Sun, K.; Wang, X.I.A.; Sprott, J.C. Bifurcations and chaos in fractional-order simplified Lorenz system. *Int. J. Bifurc. Chaos* **2010**, *20*, 1209–1219. [\[CrossRef\]](#)
19. Jafari, S.; Sprott, J.C. Simple chaotic flows with a line equilibrium. *Chaos Solitons Fractals* **2013**, *57*, 79–84. [\[CrossRef\]](#)
20. Leonov, G.A.; Kuznetsov, N.V.; Mokaev, T.N. Homoclinic orbits, and self-excited and hidden attractors in a Lorenz-like system describing convective fluid motion, Homoclinic orbits, and self-excited and hidden attractors. *Eur. Phys. J.-Spec. Top.* **2015**, *224*, 1421–1458. [\[CrossRef\]](#)
21. Bao, H.; Wang, N.; Bao, B.; Chen, M.; Jin, P.; Wang, G. Initial condition-dependent dynamics and transient period in memristor-based hypogenetic jerk system with four line equilibria. *Commun. Nonlinear Sci. Numer. Simul.* **2018**, *57*, 264–275. [\[CrossRef\]](#)
22. Suykens, J.A.; Vandewalle, J. Generation of n-double scrolls. *IEEE Trans. Circuits Syst. I* **1993**, *40*, 861–867. [\[CrossRef\]](#)
23. Yu, S.; Lu, J.; Leung, H.; Chen, G. Design and implementation of n-scroll chaotic attractors from a general jerk circuit. *IEEE Trans. Circuits Syst. I-Regul. Pap.* **2005**, *52*, 1459–1476.
24. Yu, S.; Tang, W.K.; Lu, J.; Chen, G. Generation of nxm-wing Lorenz-like attractors from a modified Shimizu-Morioka model. *IEEE Trans. Circuits Syst. II-Express Briefs* **2008**, *55*, 1168–1172.
25. Yu, S.; Jinhu, L.; Chen, G.; Yu, X. Design and implementation of grid multiwing butterfly chaotic attractors from a piecewise Lorenz system. *IEEE Trans. Circuits Syst. II-Express Briefs* **2010**, *57*, 803–807. [\[CrossRef\]](#)
26. Yu, S.; Lu, J.; Chen, G.; Yu, X. Generating grid multiwing chaotic attractors by constructing heteroclinic loops into switching systems. *IEEE Trans. Circuits Syst. II-Express Briefs* **2011**, *58*, 314–318. [\[CrossRef\]](#)
27. Huang, Y.; Zhang, P.; Zhao, W. Novel grid multiwing butterfly chaotic attractors and their circuit design. *IEEE Trans. Circuits Syst. II-Express Briefs* **2014**, *62*, 496–500. [\[CrossRef\]](#)
28. Tahir, F.R.; Jafari, S.; Pham, V.T.; Volos, C.; Wang, X. A novel no-equilibrium chaotic system with multiwing butterfly attractors. *Int. J. Bifurc. Chaos* **2015**, *25*, 1550056. [\[CrossRef\]](#)

29. Hong, Q.; Li, Y.; Wang, X.; Zeng, Z. A versatile pulse control method to generate arbitrary multidirection multibutterfly chaotic attractors. *IEEE Trans. Comput-Aided Des. Integr. Circuits Syst.* **2018**, *38*, 1480–1492. [[CrossRef](#)]
30. Ye, X.; Wang, X.; Gao, S.; Mou, J.; Wang, Z. A new random diffusion algorithm based on the multi-scroll Chua's chaotic circuit system. *Opt. Lasers Eng.* **2020**, *127*, 105905. [[CrossRef](#)]
31. Rajagopal, K.; Çiçek, S.; Naseradinmousavi, P.; Khalaf, A.J.M.; Jafari, S.; Karthikeyan, A. A novel parametrically controlled multi-scroll chaotic attractor along with electronic circuit design. *Eur. Phys. J. Plus* **2018**, *133*, 354. [[CrossRef](#)]
32. Wang, N.; Li, C.; Bao, H.; Chen, M.; Bao, B. Generating multi-scroll Chua's attractors via simplified piecewise-linear Chua's diode. *IEEE Trans. Circuits Syst. I-Regul. Pap.* **2019**, *66*, 4767–4779. [[CrossRef](#)]
33. Liu, H.; He, P.; Li, G.; Xu, X.; Zhong, H. Multi-directional annular multi-wing chaotic system based on Julia fractals. *Chaos Solitons Fractals* **2022**, *165*, 112799. [[CrossRef](#)]
34. Wang, N.; Zhang, G.; Kuznetsov, N.V.; Li, H. Generating grid chaotic sea from system without equilibrium point. *Commun. Nonlinear Sci. Numer. Simul.* **2022**, *107*, 106194. [[CrossRef](#)]
35. Wu, Q.; Hong, Q.; Liu, X.; Wang, X.; Zeng, Z. Constructing multi-butterfly attractors based on Sprott C system via non-autonomous approaches. *Chaos* **2019**, *29*, 043112. [[CrossRef](#)] [[PubMed](#)]
36. Ma, J.; Wu, X.; Chu, R.; Zhang, L. Selection of multi-scroll attractors in Jerk circuits and their verification using Pspice. *Nonlinear Dyn.* **2014**, *76*, 1951–1962. [[CrossRef](#)]
37. Hong, Q.; Wu, Q.; Wang, X.; Zeng, Z. Novel nonlinear function shift method for generating multiscroll attractors using memristor-based control circuit. *IEEE Trans. Very Large Scale Integr. (VLSI) Syst.* **2019**, *27*, 1174–1185. [[CrossRef](#)]
38. Zaamoune, F.; Menacer, T.; Lozi, R.; Chen, G. Symmetries in hidden bifurcation routes to multiscroll chaotic attractors generated by saturated function series. *J. Adv. Eng. Comput.* **2019**, *3*, 511–522. [[CrossRef](#)]
39. He, S.B.; Sun, K.H.; Zhu, C.X. Complexity analyses of multi-wing chaotic systems. *Chin. Phys. B* **2013**, *22*, 050506. [[CrossRef](#)]
40. Zhang, S.; Li, C.; Zheng, J.; Wang, X.; Zeng, Z.; Chen, G. Generating any number of diversified hidden attractors via memristor coupling. *IEEE Trans. Circuits Syst. I-Regul. Pap.* **2021**, *68*, 4945–4956. [[CrossRef](#)]
41. Yang, Y.; Huang, L.; Xiang, J.; Guo, Q. Three-dimensional sine chaotic system with multistability and multi-scroll attractor. *IEEE Trans. Circuits Syst. II-Express Briefs* **2021**, *69*, 1792–1796. [[CrossRef](#)]
42. Yan, D.; Ji'e, M.; Wang, L.; Duan, S.; Du, X. Generating novel multi-scroll chaotic attractors via fractal transformation. *Nonlinear Dyn.* **2022**, *107*, 3919–3944. [[CrossRef](#)]
43. Deng, Q.; Wang, C.; Yang, L. Four-wing hidden attractors with one stable equilibrium point. *Int. J. Bifurc. Chaos* **2020**, *30*, 2050086. [[CrossRef](#)]
44. Sahoo, S.; Roy, B.K. Design of multi-wing chaotic systems with higher largest Lyapunov exponent. *Chaos Solitons Fractals* **2022**, *157*, 111926. [[CrossRef](#)]
45. Liu, X.; Tong, X.; Wang, Z.; Zhang, M. Construction of controlled multi-scroll conservative chaotic system and its application in color image encryption. *Nonlinear Dyn.* **2022**, *110*, 1897–1934. [[CrossRef](#)]
46. Yan, S.; Li, L.; Gu, B.; Cui, Y.; Wang, J.; Song, J. Design of hyperchaotic system based on multi-scroll and its encryption algorithm in color image. *Integration* **2023**, *88*, 203–221. [[CrossRef](#)]
47. Zhang, X.; Wang, C. A novel multi-attractor period multi-scroll chaotic integrated circuit based on CMOS wide adjustable CCCII. *IEEE Access* **2019**, *7*, 16336–16350. [[CrossRef](#)]
48. Strukov, D.B.; Snider, G.S.; Stewart, D.R.; Williams, R.S. The missing memristor found. *Nature* **2008**, *453*, 80–83. [[CrossRef](#)]
49. Adhikari, S.P.; Sah, M.P.; Kim, H.; Chua, L.O. Three fingerprints of memristor. *IEEE Trans. Circuits Syst. I-Regul. Pap.* **2013**, *60*, 3008–3021. [[CrossRef](#)]
50. Chua, L. Everything you wish to know about memristors but are afraid to ask. *Radioengineering* **2015**, *24*, 319–368. [[CrossRef](#)]
51. Muthuswamy, B.; Kokate, P.P. Memristor-based chaotic circuits. *IETE Tech. Rev.* **2009**, *26*, 417–429. [[CrossRef](#)]
52. Cafagna, D.; Grassi, G. On the simplest fractional-order memristor-based chaotic system. *Nonlinear Dyn.* **2012**, *70*, 1185–1197. [[CrossRef](#)]
53. Lai, Q.; Wan, Z.; Kengne, L.K.; Kuate, P.D.K.; Chen, C. Two-memristor-based chaotic system with infinite coexisting attractors. *IEEE Trans. Circuits Syst. II-Express Briefs* **2020**, *68*, 2197–2201. [[CrossRef](#)]
54. Chang, H.; Li, Y.; Chen, G.; Yuan, F. Extreme multistability and complex dynamics of a memristor-based chaotic system. *Int. J. Bifurc. Chaos* **2020**, *30*, 2030019. [[CrossRef](#)]
55. Butusov, D.N.; Ostrovskii, V.Y.; Karimov, A.I.; Andreev, V.S. Semi-explicit composition methods in memcapacitor circuit simulation. *Int. J. Embed. Real-Time Commun. Syst.* **2019**, *10*, 37–52. [[CrossRef](#)]
56. Ostrovskii, V.Y.; Tutueva, A.V.; Rybin, V.G.; Karimov, A.I.; Butusov, D.N. Continuation analysis of memristor-based modified Chua's circuit. In Proceedings of the 2020 International Conference Nonlinearity, Information and Robotics (NIR), Innopolis, Russia, 3–6 December 2020; IEEE: Piscataway, NJ, USA, 2020; pp. 1–5.
57. Xu, Q.; Lin, Y.; Bao, B.; Chen, M. Multiple attractors in a non-ideal active voltage-controlled memristor based Chua's circuit. *Chaos Solitons Fractals* **2016**, *83*, 186–200. [[CrossRef](#)]
58. Chen, M.; Sun, M.; Bao, H.; Hu, Y.; Bao, B. Flux–charge analysis of two-memristor-based Chua's circuit, dimensionality decreasing model for detecting extreme multistability. *IEEE Trans. Ind. Electron.* **2019**, *67*, 2197–2206. [[CrossRef](#)]
59. Kengne, J.; Negou, A.N.; Tchiotso, D. Antimonotonicity, chaos and multiple attractors in a novel autonomous memristor-based jerk circuit. *Nonlinear Dyn.* **2017**, *88*, 2589–2608. [[CrossRef](#)]

60. Hua, M.; Yang, S.; Xu, Q.; Chen, M.; Wu, H.; Bao, B. Forward and reverse asymmetric memristor-based jerk circuits. *AEU-Int. J. Electron. Commun.* **2020**, *123*, 153294. [[CrossRef](#)]
61. Bao, H.; Ding, R.; Hua, M.; Wu, H.; Chen, B. Initial-condition effects on a two-memristor-based Jerk system. *Mathematics* **2022**, *10*, 411. [[CrossRef](#)]
62. Xu, Q.; Cheng, S.; Ju, Z.; Chen, M.; Wu, H. Asymmetric coexisting bifurcations and multi-stability in an asymmetric memristive diode-bridge-based jerk circuit. *Chin. J. Phys.* **2021**, *70*, 69–81. [[CrossRef](#)]
63. Bao, B.; Ma, Z.; Xu, J.; Liu, Z.; Xu, Q. A simple memristor chaotic circuit with complex dynamics. *Int. J. Bifurc. Chaos* **2011**, *21*, 2629–2645. [[CrossRef](#)]
64. Dou, G.; Yang, H.; Gao, Z.; Li, P.; Dou, M.; Yang, W.; Guo, M.; Li, Y. Coexisting multi-dynamics of a physical SBT memristor-based chaotic circuit. *Int. J. Bifurc. Chaos* **2020**, *30*, 2030043. [[CrossRef](#)]
65. Muthuswamy, B. Implementing memristor based chaotic circuits. *Int. J. Bifurc. Chaos* **2010**, *20*, 1335–1350. [[CrossRef](#)]
66. Jiang, Y.; Li, C.; Liu, Z.; Lei, T.; Chen, G. Simplified memristive Lorenz oscillator. *IEEE Trans. Circuits Syst. II-Express Briefs* **2022**, *69*, 3344–3348. [[CrossRef](#)]
67. Ramamoorthy, R.; Rajagopal, K.; Leutcho, G.D.; Krejcar, O.; Namazi, H.; Hussain, I. Multistable dynamics and control of a new 4D memristive chaotic Sprott B system. *Chaos Solitons Fractals* **2022**, *156*, 111834. [[CrossRef](#)]
68. Li, C.; Sprott, J.C.; Joo-Chen Thio, W.; Gu, Z. A simple memristive jerk system. *IET Circ. Devices Syst.* **2021**, *15*, 388–392. [[CrossRef](#)]
69. Jia, S.H.; Li, Y.X.; Shi, Q.Y.; Huang, X. Design and FPGA implementation of a memristor-based multi-scroll hyperchaotic system. *Chin. Phys. B* **2022**, *31*, 070505. [[CrossRef](#)]
70. Alombah, N.H.; Fotsin, H.; Ngouonkadi, E.M.; Nguazon, T. Dynamics, analysis and implementation of a multiscroll memristor-based chaotic circuit. *Int. J. Bifurc. Chaos* **2016**, *26*, 1650128. [[CrossRef](#)]
71. Yuan, F.; Wang, G.; Wang, X. Extreme multistability in a memristor-based multi-scroll hyper-chaotic system. *Chaos* **2016**, *26*, 073107. [[CrossRef](#)]
72. Zhang, S.; Zheng, J.; Wang, X.; Zeng, Z.; Peng, X. A novel nonideal flux-controlled memristor model for generating arbitrary multi-double-scroll and multi-double-wing attractors. *Int. J. Bifurc. Chaos* **2021**, *31*, 2150086. [[CrossRef](#)]
73. Zhang, S.; Zheng, J.; Wang, X.; Zeng, Z. Multi-scroll hidden attractor in memristive HR neuron model under electromagnetic radiation and its applications. *Chaos* **2021**, *31*, 011101. [[CrossRef](#)] [[PubMed](#)]
74. Gu, S.; Peng, Q.; Leng, X.; Du, B. A novel non-equilibrium memristor-based system with multi-wing attractors and multiple transient transitions. *Chaos* **2021**, *31*, 033105. [[CrossRef](#)] [[PubMed](#)]
75. Guo, Z.; Wen, J.; Mou, J. Dynamic analysis and DSP implementation of memristor chaotic systems with multiple forms of hidden attractors. *Mathematics* **2023**, *11*, 24. [[CrossRef](#)]
76. Chang, H.; Li, Y.; Chen, G. A novel memristor-based dynamical system with multi-wing attractors and symmetric periodic bursting. *Chaos* **2020**, *30*, 043110. [[CrossRef](#)] [[PubMed](#)]
77. Hu, X.; Liu, C.; Liu, L.; Yao, Y.; Zheng, G. Multi-scroll hidden attractors and multi-wing hidden attractors in a 5-dimensional memristive system. *Chin. Phys. B* **2017**, *26*, 110502. [[CrossRef](#)]
78. Yan, D.; Wang, L.; Duan, S.; Chen, J.; Chen, J. Chaotic attractors generated by a memristor-based chaotic system and Julia fractal. *Chaos Solitons Fractals* **2021**, *146*, 110773. [[CrossRef](#)]
79. Xu, Q.; Ding, S.; Bao, H.; Chen, M.; Bao, B. Piecewise-linear simplification for adaptive synaptic neuron model. *IEEE Trans. Circuits Syst. II-Express Briefs* **2021**, *69*, 1832–1836. [[CrossRef](#)]
80. Ma, M.; Lu, Y.; Li, Z.; Sun, Y.; Wang, C. Multistability and phase synchronization of Rulkov neurons coupled with a locally active discrete memristor. *Fractal Fract.* **2023**, *7*, 82. [[CrossRef](#)]
81. Li, H.; Yang, Y.; Li, W.; He, S.; Li, C. Extremely rich dynamics in a memristor-based chaotic system. *Eur. Phys. J. Plus* **2020**, *135*, 579. [[CrossRef](#)]
82. Zhang, Y.; Liu, Z.; Wu, H.; Chen, S.; Bao, B. Two-memristor-based chaotic system and its extreme multistability reconstitution via dimensionality reduction analysis. *Chaos Solitons Fractals* **2019**, *127*, 354–363. [[CrossRef](#)]
83. Li, C.; Min, F.; Li, C. Multiple coexisting attractors of the serial-parallel memristor-based chaotic system and its adaptive generalized synchronization. *Nonlinear Dyn.* **2018**, *94*, 2785–2806. [[CrossRef](#)]
84. Ding, D.; Qian, X.; Hu, W.; Wang, N.; Liang, D. Chaos and Hopf bifurcation control in a fractional-order memristor-based chaotic system with time delay. *Eur. Phys. J. Plus* **2017**, *132*, 447. [[CrossRef](#)]
85. Wu, J.; Wang, L.; Chen, G.; Duan, S. A memristive chaotic system with heart-shaped attractors and its implementation. *Chaos Solitons Fractals* **2016**, *92*, 20–29. [[CrossRef](#)]
86. Wang, X.; Zhang, X.; Gao, M.; Tian, Y.; Wang, C.; Iu, H.H.C. A color image encryption algorithm based on hash table, hilbert curve and hyper-chaotic synchronization. *Mathematics* **2023**, *11*, 567. [[CrossRef](#)]
87. Wang, R.; Li, C.; Kong, S.; Jiang, Y.; Lei, T. A 3D memristive chaotic system with conditional symmetry. *Chaos Solitons Fractals* **2022**, *158*, 111992. [[CrossRef](#)]
88. Mezatio, B.A.; Motchongom, M.T.; Tekam, B.R.W.; Kengne, R.; Tchitnga, R.; Fomethé, A. A novel memristive 6D hyperchaotic autonomous system with hidden extreme multistability. *Chaos Solitons Fractals* **2019**, *120*, 100–115. [[CrossRef](#)]
89. Ma, M.; Yang, Y.; Qiu, Z.; Peng, Y.; Sun, Y.; Li, Z.; Wang, M. A locally active discrete memristor model and its application in a hyperchaotic map. *Nonlinear Dyn.* **2022**, *107*, 2935–2949. [[CrossRef](#)]

90. Jin, J.; Cui, L. Fully integrated memristor and its application on the scroll-controllable hyperchaotic system. *Complexity* **2019**, *2019*, 4106398. [[CrossRef](#)]
91. Rajagopal, K.; Vaidyanathan, S.; Karthikeyan, A.; Srinivasan, A. Complex novel 4D memristor hyperchaotic system and its synchronization using adaptive sliding mode control. *Alex. Eng. J.* **2018**, *57*, 683–694. [[CrossRef](#)]
92. Wan, Q.; Zhou, Z.; Ji, W.; Wang, C.; Yu, F. Dynamic analysis and circuit realization of a novel no-equilibrium 5D memristive hyperchaotic system with hidden extreme multistability. *Complexity* **2020**, *2020*, 7106861. [[CrossRef](#)]
93. Li, H.; Hua, Z.; Bao, H.; Zhu, L.; Chen, M.; Bao, B. Two-dimensional memristive hyperchaotic maps and application in secure communication. *IEEE Trans. Ind. Electron.* **2020**, *68*, 9931–9940. [[CrossRef](#)]
94. Lai, Q.; Yang, L.; Liu, Y. Design and realization of discrete memristive hyperchaotic map with application in image encryption. *Chaos Solitons Fractals* **2022**, *165*, 112781. [[CrossRef](#)]
95. Yu, F.; Xu, S.; Xiao, X.; Yao, W.; Huang, Y.; Cai, S.; Yin, B.; Li, Y. Dynamics analysis, FPGA realization and image encryption application of a 5D memristive exponential hyperchaotic system. *Integration* **2023**, *90*, 58–70. [[CrossRef](#)]
96. Ma, M.; Xiong, K.; Li, Z.; Sun, Y. Dynamic behavior analysis and synchronization of memristor-coupled heterogeneous discrete neural network. *Mathematics* **2023**, *11*, 375. [[CrossRef](#)]
97. Li, C.; Lei, T.; Liu, Z. Offset parameter cancellation produces countless coexisting attractors. *Chaos* **2022**, *32*, 121104. [[CrossRef](#)] [[PubMed](#)]
98. Zhou, C.; Wang, C.; Yao, W.; Lin, H. Observer-based synchronization of memristive Neural Network under DoS attacks and actuator saturation and its application to image encryption. *Appl. Math. Comput.* **2022**, *425*, 127080. [[CrossRef](#)]
99. Hopfield, J.J. Neurons with graded response have collective computational properties like those of two-state neurons. *Proc. Natl. Acad. Sci. Belarus-Agrar. Ser.* **1984**, *81*, 3088–3092. [[CrossRef](#)] [[PubMed](#)]
100. Das, A.; Das, P.; Roy, A.B. Chaos in a three-dimensional general model of neural network. *Int. J. Bifurc. Chaos* **2002**, *12*, 2271–2281. [[CrossRef](#)]
101. Aram, Z.; Jafari, S.; Ma, J.; Sprott, J.C.; Zendehtrouh, S.; Pham, V.T. Using chaotic artificial neural networks to model memory in the brain. *Commun. Nonlinear Sci. Numer. Simul.* **2017**, *44*, 449–459. [[CrossRef](#)]
102. Liu, L.; Zhang, L.; Jiang, D.; Guan, Y.; Zhang, Z. A simultaneous scrambling and diffusion color image encryption algorithm based on Hopfield chaotic neural network. *IEEE Access* **2019**, *7*, 185796–185810. [[CrossRef](#)]
103. Yi, S.I.; Kumar, S.; Williams, R.S. Improved hopfield network optimization using manufacturable three-terminal electronic synapses. *IEEE Trans. Circuits Syst. I-Regul. Pap.* **2021**, *68*, 4970–4978. [[CrossRef](#)]
104. Bao, B.; Chen, C.; Bao, H.; Zhang, X.; Xu, Q.; Chen, M. Dynamical effects of neuron activation gradient on Hopfield neural network, numerical analyses and hardware experiments. *Int. J. Bifurc. Chaos* **2019**, *29*, 1930010. [[CrossRef](#)]
105. Lin, H.; Wang, C.; Chen, C.; Sun, Y.; Zhou, C.; Xu, C.; Hong, Q. Neural bursting and synchronization emulated by neural network and circuits. *IEEE Trans. Circuits Syst. I-Regul. Pap.* **2021**, *68*, 3397–3410. [[CrossRef](#)]
106. Tabekoueng Njitacke, Z.; Laura Matze, C.; Fouodji Tsotsop, M.; Kengne, J. Remerging feigenbaum trees, coexisting behaviors and bursting oscillations in a novel 3D generalized Hopfield neural network. *Neural Process. Lett.* **2020**, *52*, 267–289. [[CrossRef](#)]
107. Ma, J. Biophysical neurons, energy, and synapse controllability: A review. *J. Zhejiang Univ.-Sci. A* **2023**, *24*, 109–129. [[CrossRef](#)]
108. Lin, H.; Wang, C.; Deng, Q.; Xu, C.; Deng, Z.; Zhou, C. Review on chaotic dynamics of memristive neuron and neural network. *Nonlinear Dyn.* **2021**, *106*, 959–973. [[CrossRef](#)]
109. Wu, F.; Wang, C.; Jin, W.; Ma, J. Dynamical responses in a new neuron model subjected to electromagnetic induction and phase noise. *Phys. A* **2017**, *469*, 81–88. [[CrossRef](#)]
110. Lv, M.; Wang, C.; Ren, G.; Ma, J.; Song, X. Model of electrical activity in a neuron under magnetic flow effect. *Nonlinear Dyn.* **2016**, *85*, 1479–1490. [[CrossRef](#)]
111. Li, Q.; Tang, S.; Zeng, H.; Zhou, T. On hyperchaos in a small memristive neural network. *Nonlinear Dyn.* **2014**, *78*, 1087–1099. [[CrossRef](#)]
112. Pham, V.T.; Jafari, S.; Vaidyanathan, S.; Volos, C.; Wang, X. A novel memristive neural network with hidden attractors and its circuitry implementation. *China-Technol. Sci.* **2016**, *59*, 358–363. [[CrossRef](#)]
113. Bao, B.; Qian, H.; Xu, Q.; Chen, M.; Wang, J.; Yu, Y. Coexisting behaviors of asymmetric attractors in hyperbolic-type memristor based Hopfield neural network. *Front. Comput. Neurosci.* **2017**, *11*, 81. [[CrossRef](#)] [[PubMed](#)]
114. Hu, X.; Liu, C.; Liu, L.; Ni, J.; Yao, Y. Chaotic dynamics in a neural network under electromagnetic radiation. *Nonlinear Dyn.* **2018**, *91*, 1541–1554. [[CrossRef](#)]
115. Lin, H.; Wang, C.; Hong, Q.; Sun, Y. A multi-stable memristor and its application in a neural network. *IEEE Trans. Circuits Syst. II-Express Briefs* **2020**, *67*, 3472–3476. [[CrossRef](#)]
116. Zhang, S.; Zheng, J.; Wang, X.; Zeng, Z.; He, S. Initial offset boosting coexisting attractors in memristive multi-double-scroll Hopfield neural network. *Nonlinear Dyn.* **2020**, *102*, 2821–2841. [[CrossRef](#)]
117. Lin, H.; Wang, C.; Xu, C.; Zhang, X.; Iu, H.H. A memristive synapse control method to generate diversified multi-structure chaotic attractors. *IEEE Trans. Comput-Aided Des. Integr. Circuits Syst.* **2023**, *42*, 942–955. [[CrossRef](#)]
118. Lin, H.; Wang, C.; Sun, J.; Zhang, X.; Sun, Y.; Iu, H.H. Memristor-coupled asymmetric neural network, bionic modeling, chaotic dynamics analysis and encryption application. *Chaos Solitons Fractals* **2023**, *166*, 112905. [[CrossRef](#)]
119. Xu, S.; Wang, X.; Ye, X. A new fractional-order chaos system of Hopfield neural network and its application in image encryption. *Chaos Solitons Fractals* **2022**, *157*, 111889. [[CrossRef](#)]
120. Yu, F.; Shen, H.; Yu, Q.; Kong, X.; Sharma, P.K.; Cai, S. Privacy protection of medical data based on multi-scroll memristive Hopfield neural network. *IEEE Trans. Netw. Sci. Eng.* **2023**, *10*, 845–858. [[CrossRef](#)]

121. Lin, H.; Wang, C.; Cui, L.; Sun, Y.; Xu, C.; Yu, F. Brain-like initial-boosted hyperchaos and application in biomedical image encryption. *IEEE Trans. Ind. Inform.* **2022**, *18*, 8839–8850. [[CrossRef](#)]
122. Yu, F.; Chen, H.; Kong, X.; Yu, Q.; Cai, S.; Huang, Y.; Du, S. Dynamic analysis and application in medical digital image watermarking of a new multi-scroll neural network with quartic nonlinear memristor. *Eur. Phys. J. Plus* **2022**, *137*, 434. [[CrossRef](#)] [[PubMed](#)]
123. Lin, H.; Wang, C.; Cui, L.; Sun, Y.; Zhang, X.; Yao, W. Hyperchaotic memristive ring neural network and application in medical image encryption. *Nonlinear Dyn.* **2022**, *110*, 841–855. [[CrossRef](#)]
124. Kandel, E.R.; Schwartz, J.H.; Jessell, T.M.; Siegelbaum, S.; Hudspeth, A.J.; Mack, S. (Eds.) *Principles of Neural Science*; McGraw-hill: New York, NY, USA, 2000; Volume 4, pp. 1227–1246.
125. Chen, C.; Min, F.; Zhang, Y.; Bao, H. ReLU-type Hopfield neural network with analog hardware implementation. *Chaos Solitons Fractals* **2023**, *167*, 113068. [[CrossRef](#)]
126. Wang, H.; Yu, Y.; Wen, G.; Zhang, S.; Yu, J. Global stability analysis of fractional-order Hopfield neural network with time delay. *Neurocomputing* **2015**, *154*, 15–23. [[CrossRef](#)]
127. Debbouche, N.; Ouannas, A.; Batiha, I.M.; Grassi, G.; Kaabar, M.K.; Jahanshahi, H.; Aly, A.A.; Aljuaid, A.M. Chaotic behavior analysis of a new incommensurate fractional-order hopfield neural network system. *Complexity* **2021**, *2021*, 3394666. [[CrossRef](#)]
128. Ma, C.; Mou, J.; Yang, F.; Yan, H. A fractional-order hopfield neural network chaotic system and its circuit realization. *Eur. Phys. J. Plus* **2020**, *135*, 100. [[CrossRef](#)]
129. Karim, S.A.; Zamri, N.E.; Alway, A.; Kasihmuddin, M.S.M.; Ismail, A.I.M.; Mansor, M.A.; Hassan, N.F.A. Random satisfiability, A higher-order logical approach in discrete Hopfield neural network. *IEEE Access* **2021**, *9*, 50831–50845. [[CrossRef](#)]
130. Rebentrost, P.; Bromley, T.R.; Weedbrook, C.; Lloyd, S. Quantum Hopfield neural network. *Phys. Rev. A* **2018**, *98*, 042308. [[CrossRef](#)]
131. Barra, A.; Beccaria, M.; Fachechi, A. A new mechanical approach to handle generalized Hopfield neural network. *Neural Netw.* **2018**, *106*, 205–222. [[CrossRef](#)]
132. Chua, L. Memristor—the missing circuit element. *IEEE Trans. Circuit Theory* **1971**, *18*, 507–519. [[CrossRef](#)]
133. Liao, M.; Wang, C.; Sun, Y.; Lin, H.; Xu, C. Memristor-based affective associative memory neural network circuit with emotional gradual processes. *Neural Comput. Appl.* **2022**, *34*, 13667–13682. [[CrossRef](#)]
134. Tan, Y.; Wang, C. A simple locally active memristor and its application in HR neurons. *Chaos* **2020**, *30*, 053118. [[CrossRef](#)] [[PubMed](#)]
135. Deng, Z.; Wang, C.; Lin, H.; Sun, Y. A memristive spiking neural network circuit with selective supervised attention algorithm. In *IEEE Transactions on Computer-Aided Design of Integrated Circuits and Systems*; IEEE: Piscataway, NJ, USA, 2023. [[CrossRef](#)]
136. Li, Y.; Wang, Z.; Midya, R.; Xia, Q.; Yang, J.J. Review of memristor devices in neuromorphic computing, materials sciences and device challenges. *J. Phys. D-Appl. Phys.* **2018**, *51*, 503002. [[CrossRef](#)]
137. Hong, Q.; Shi, Z.; Sun, J.; Du, S. Memristive self-learning logic circuit with application to encoder and decoder. *Neural Comput. Appl.* **2021**, *33*, 4901–4913. [[CrossRef](#)]
138. Wen, Z.; Wang, C.; Deng, Q.; Lin, H. Regulating memristive neuronal dynamical properties via excitatory or inhibitory magnetic field coupling. *Nonlinear Dyn.* **2022**, *110*, 3823–3835. [[CrossRef](#)]
139. Lv, M.; Ma, J. Multiple modes of electrical activities in a new neuron model under electromagnetic radiation. *Neurocomputing* **2016**, *205*, 375–381. [[CrossRef](#)]
140. Xu, Q.; Ju, Z.; Ding, S.; Feng, C.; Chen, M.; Bao, B. Electromagnetic induction effects on electrical activity within a memristive Wilson neuron model. *Cogn. Neurodynamics* **2022**, *16*, 1221–1231. [[CrossRef](#)]
141. Zhou, C.; Wang, C.; Sun, Y.; Yao, W.; Lin, H. Cluster output synchronization for memristive neural network. *Inf. Sci.* **2022**, *589*, 459–477. [[CrossRef](#)]
142. Lu, Y.; Wang, C.; Deng, Q. Rulkov neural network coupled with discrete memristors. *Networks* **2022**, *33*, 214–232. [[CrossRef](#)]
143. Faradja, P.; Qi, G. Analysis of multistability, hidden chaos and transient chaos in brushless DC motor. *Chaos Solitons Fractals* **2020**, *132*, 109606. [[CrossRef](#)]
144. Chen, M.; Li, M.; Yu, Q.; Bao, B.; Xu, Q.; Wang, J. Dynamics of self-excited attractors and hidden attractors in generalized memristor-based Chua’s circuit. *Nonlinear Dyn.* **2015**, *81*, 215–226. [[CrossRef](#)]
145. Jafari, S.; Rajagopal, K.; Hayat, T.; Alsaedi, A.; Pham, V.T. Simplest megastable chaotic oscillator. *Int. J. Bifurc. Chaos* **2019**, *29*, 1950187. [[CrossRef](#)]
146. Gu, S.; He, S.; Wang, H.; Du, B. Analysis of three types of initial offset-boosting behavior for a new fractional-order dynamical system. *Chaos Solitons Fractals* **2021**, *143*, 110613. [[CrossRef](#)]
147. Njitacke, Z.T.; Kengne, J.; Fotsin, H.B. A plethora of behaviors in a memristor based Hopfield neural network. *Int. J. Dyn. Syst. Cont.* **2019**, *7*, 36–52. [[CrossRef](#)]
148. Xu, Q.; Song, Z.; Bao, H.; Chen, M.; Bao, B. Two-neuron-based non-autonomous memristive Hopfield neural network, numerical analyses and hardware experiments. *AEU-Int. J. Electron. Commun.* **2018**, *96*, 66–74. [[CrossRef](#)]
149. Li, R.; Dong, E.; Tong, J.; Wang, Z. A novel multiscroll memristive Hopfield neural network. *Int. J. Bifurc. Chaos* **2022**, *32*, 2250130. [[CrossRef](#)]
150. Lai, Q.; Wan, Z.; Zhang, H.; Chen, G. Design and analysis of multiscroll memristive hopfield neural network with adjustable memductance and application to image encryption. In *IEEE Transactions on Neural Networks and Learning Systems*; IEEE: Piscataway, NJ, USA, 2022. [[CrossRef](#)]

151. Hua, M.; Bao, H.; Wu, H.; Xu, Q.; Bao, B. A single neuron model with memristive synaptic weight. *Chin. J. Phys.* **2022**, *76*, 217–227. [[CrossRef](#)]
152. Doubla, I.S.; Ramakrishnan, B.; Njitacke, Z.T.; Kengne, J.; Rajagopal, K. Hidden extreme multistability and its control with selection of a desired attractor in a non-autonomous Hopfield neuron. *AEU-Int. J. Electron. Commun.* **2022**, *144*, 154059. [[CrossRef](#)]
153. Doubla, I.S.; Ramakrishnan, B.; Tabekoueng, Z.N.; Kengne, J.; Rajagopal, K. Infinitely many coexisting hidden attractors in a new hyperbolic-type memristor-based HNN. *Eur. Phys. J.-Spec. Top.* **2022**, *231*, 2371–2385. [[CrossRef](#)]
154. Bao, H.; Hua, M.; Ma, J.; Chen, M.; Bao, B. Offset-control plane coexisting behaviors in two-memristor-based Hopfield neural network. In *IEEE Transactions on Industrial Electronics*; IEEE: Piscataway, NJ, USA, 2022. [[CrossRef](#)]
155. Shen, H.; Yu, F.; Kong, X.; Mokbel, A.A.M.; Wang, C.; Cai, S. Dynamics study on the effect of memristive autapse distribution on Hopfield neural network. *Chaos* **2022**, *32*, 083133. [[CrossRef](#)] [[PubMed](#)]
156. Parastesh, F.; Jafari, S.; Azarnoush, H.; Hatef, B.; Namazi, H.; Dudkowski, D. Chimera in a network of memristor-based Hopfield neural network. *Eur. Phys. J.-Spec. Top.* **2019**, *228*, 2023–2033. [[CrossRef](#)]
157. Ding, D.; Luo, J.; Shan, X.; Hu, Y.; Yang, Z.; Ding, L. Coexisting behaviors of a fraction-order novel hyperbolic-type memristor Hopfield neuron network based on three neurons. *Int. J. Mod. Phys. B* **2020**, *34*, 2050302. [[CrossRef](#)]
158. Wang, Z.; Parastesh, F.; Rajagopal, K.; Hamarash, I.I.; Hussain, I. Delay-induced synchronization in two coupled chaotic memristive Hopfield neural network. *Chaos Solitons Fractals* **2020**, *134*, 109702. [[CrossRef](#)]
159. Leng, Y.; Yu, D.; Hu, Y.; Yu, S.S.; Ye, Z. Dynamic behaviors of hyperbolic-type memristor-based Hopfield neural network considering synaptic crosstalk. *Chaos* **2020**, *30*, 033108. [[CrossRef](#)] [[PubMed](#)]
160. Boya, B.F.B.A.; Kengne, J.; Kenmoe, G.D.; Effa, J.Y. Four-scroll attractor on the dynamics of a novel Hopfield neural network based on bi-neurons without bias current. *Heliyon* **2022**, *8*, e11046. [[CrossRef](#)] [[PubMed](#)]
161. Bao, H.; Chen, Z.; Cai, J.; Xu, Q.; Bao, B. Memristive cyclic three-neuron-based neural network with chaos and global coexisting attractors. *Sci. China-Technol. Sci.* **2022**, *65*, 2582–2592. [[CrossRef](#)]
162. Chen, C.; Min, F. ReLU-type memristor-based Hopfield neural network. *Eur. Phys. J.-Spec. Top.* **2022**, *231*, 2979–2992. [[CrossRef](#)]
163. Ma, T.; Mou, J.; Yan, H.; Cao, Y. A new class of Hopfield neural network with double memristive synapses and its DSP implementation. *Eur. Phys. J. Plus* **2022**, *137*, 1135. [[CrossRef](#)]
164. Lai, Q.; Wan, Z.; Kuate, P.D.K. Generating grid multi-scroll attractors in memristive neural network. *IEEE Trans. Circuits Syst. I-Regul. Pap.* **2022**, *70*, 1324–1336. [[CrossRef](#)]
165. Lai, Q.; Lai, C.; Kuate, P.D.K.; Li, C.; He, S. Chaos in a simplest cyclic memristive neural network. *Int. J. Bifurc. Chaos* **2022**, *32*, 2250042. [[CrossRef](#)]
166. Li, C.; Yang, Y.; Yang, X.; Zi, X.; Xiao, F. A tristable locally active memristor and its application in Hopfield neural network. *Nonlinear Dyn.* **2022**, *108*, 1697–1717. [[CrossRef](#)]
167. Ding, D.; Xiao, H.; Yang, Z.; Luo, H.; Hu, Y.; Zhang, X.; Liu, Y. Coexisting multi-stability of Hopfield neural network based on coupled fractional-order locally active memristor and its application in image encryption. *Nonlinear Dyn.* **2022**, *108*, 4433–4458. [[CrossRef](#)]
168. Yu, F.; Kong, X.; Mokbel, A.A.M.; Yao, W.; Cai, S. Complex dynamics, hardware implementation and image encryption application of multiscroll memristive Hopfield neural network with a novel local active memristor. *IEEE Trans. Circuits Syst. II-Express Briefs* **2022**, *70*, 326–330. [[CrossRef](#)]
169. Lin, H.; Wang, C. Influences of electromagnetic radiation distribution on chaotic dynamics of a neural network. *Appl. Math. Comput.* **2020**, *369*, 124840. [[CrossRef](#)]
170. Lin, H.; Wang, C.; Tan, Y. Hidden extreme multistability with hyperchaos and transient chaos in a Hopfield neural network affected by electromagnetic radiation. *Nonlinear Dyn.* **2020**, *99*, 2369–2386. [[CrossRef](#)]
171. Lin, H.; Wang, C.; Sun, Y.; Wang, T. Generating n-scroll chaotic attractors from a memristor-based magnetized Hopfield neural network. *IEEE Trans. Circuits Syst. II-Express Briefs* **2022**, *70*, 311–315. [[CrossRef](#)]
172. Wan, Q.; Li, F.; Chen, S.; Yang, Q. Symmetric multi-scroll attractors in magnetized Hopfield neural network under pulse controlled memristor and pulse current stimulation. *Chaos Solitons Fractals* **2023**, *169*, 113259. [[CrossRef](#)]
173. Wan, Q.; Yan, Z.; Li, F.; Liu, J.; Chen, S. Multistable dynamics in a Hopfield neural network under electromagnetic radiation and dual bias currents. *Nonlinear Dyn.* **2022**, *109*, 2085–2101. [[CrossRef](#)]
174. Lin, H.; Wang, C.; Yao, W.; Tan, Y. Chaotic dynamics in a neural network with different types of external stimuli. *Commun. Nonlinear Sci. Numer. Simul.* **2020**, *90*, 105390. [[CrossRef](#)]
175. Chen, C.; Chen, J.; Bao, H.; Chen, M.; Bao, B. Coexisting multi-stable patterns in memristor synapse-coupled Hopfield neural network with two neurons. *Nonlinear Dyn.* **2019**, *95*, 3385–3399. [[CrossRef](#)]
176. Chen, C.; Bao, H.; Chen, M.; Xu, Q.; Bao, B. Non-ideal memristor synapse-coupled bi-neuron Hopfield neural network, Numerical simulations and breadboard experiments. *AEU-Int. J. Electron. Commun.* **2019**, *111*, 152894. [[CrossRef](#)]
177. Chen, C.; Min, F.; Zhang, Y.; Bao, B. Memristive electromagnetic induction effects on Hopfield neural network. *Nonlinear Dyn.* **2021**, *106*, 2559–2576. [[CrossRef](#)]
178. Wan, Q.; Yan, Z.; Li, F.; Chen, S.; Liu, J. Complex dynamics in a Hopfield neural network under electromagnetic induction and electromagnetic radiation. *Chaos* **2022**, *32*, 073107. [[CrossRef](#)] [[PubMed](#)]
179. Eftekhari, L.; Amirian, M.M. Stability analysis of fractional order memristor synapse-coupled hopfield neural network with ring structure. *Cogn. Neurodynamics* **2022**. [[CrossRef](#)]

180. Yu, F.; Kong, X.; Chen, H.; Yu, Q.; Cai, S.; Huang, Y.; Du, S. A 6D fractional-order memristive Hopfield neural network and its application in image encryption. *Front. Phys.* **2022**, *10*, 847385. [[CrossRef](#)]
181. Dong, T.; Gong, X.; Huang, T. Zero-Hopf Bifurcation of a memristive synaptic Hopfield neural network with time delay. *Neural Netw.* **2022**, *149*, 146–156. [[CrossRef](#)]
182. Ding, S.; Wang, N.; Bao, H.; Chen, B.; Wu, H.; Xu, Q. Memristor synapse-coupled piecewise-linear simplified Hopfield neural network, Dynamics analysis and circuit implementation. *Chaos Solitons Fractals* **2023**, *166*, 112899. [[CrossRef](#)]
183. Yu, F.; Yu, Q.; Chen, H.; Kong, X.; Mokbel, A.A.M.; Cai, S.; Du, S. Dynamic analysis and audio encryption application in IoT of a multi-scroll fractional-order memristive Hopfield neural network. *Fractal Fract.* **2022**, *6*, 370. [[CrossRef](#)]
184. Hu, S.G.; Liu, Y.; Liu, Z.; Chen, T.P.; Wang, J.J.; Yu, Q.; Deng, L.J.; Yin, Y.; Hosaka, S. Associative memory realized by a reconfigurable memristive Hopfield neural network. *Nat. Commun.* **2015**, *6*, 7522. [[CrossRef](#)]
185. Fahimi, Z.; Mahmoodi, M.R.; Nili, H.; Polishchuk, V.; Strukov, D.B. Combinatorial optimization by weight annealing in memristive hopfield networks. *Sci. Rep.* **2021**, *11*, 16383. [[CrossRef](#)] [[PubMed](#)]
186. Li, R.; Ding, R. A novel locally active time-delay memristive Hopfield neural network and its application. *Eur. Phys. J.-Spec. Top.* **2022**, *231*, 3005–3017. [[CrossRef](#)]
187. Hong, Q.; Yan, R.; Wang, C.; Sun, J. Memristive circuit implementation of biological nonassociative learning mechanism and its applications. *IEEE Trans. Biomed. Circuits Syst.* **2020**, *14*, 1036–1050. [[CrossRef](#)] [[PubMed](#)]
188. Wang, C.; Xu, C.; Sun, J.; Deng, Q. A memristor-based associative memory neural network circuit with emotion effect. *Neural Comput. Applic.* **2023**. [[CrossRef](#)]
189. Sun, J.; Kang, K.; Sun, Y.; Hong, Q.; Wang, C. A multi-value 3D crossbar array nonvolatile memory based on pure memristors. *Eur. Phys. J.-Spec. Top.* **2022**, *231*, 3119–3130. [[CrossRef](#)]
190. Huang, L.L.; Zhang, Y.; Xiang, J.H.; Liu, J. Extreme multistability in a Hopfield neural network based on two biological neuronal systems. *IEEE Trans. Circuits Syst. II-Express Briefs* **2022**, *69*, 4568–4572. [[CrossRef](#)]
191. Ostrovskii, V.; Fedoseev, P.; Bobrova, Y.; Butusov, D. Structural and parametric identification of known memristors. *Nanomaterials* **2021**, *12*, 63. [[CrossRef](#)]
192. Yuan, F.; Li, S.; Deng, Y.; Li, Y.; Chen, G. Cu-doped TiO₂-x nanoscale memristive applications in chaotic circuit and true random number generator. *IEEE Trans. Ind. Electron.* **2022**, *70*, 4120–4127. [[CrossRef](#)]

Disclaimer/Publisher's Note: The statements, opinions and data contained in all publications are solely those of the individual author(s) and contributor(s) and not of MDPI and/or the editor(s). MDPI and/or the editor(s) disclaim responsibility for any injury to people or property resulting from any ideas, methods, instructions or products referred to in the content.